

Supplement of Atmos. Chem. Phys., 14, 12307–12317, 2014
<http://www.atmos-chem-phys.net/14/12307/2014/>
doi:10.5194/acp-14-12307-2014-supplement
© Author(s) 2014. CC Attribution 3.0 License.



Supplement of

CCN activity of size-selected aerosol at a Pacific coastal location

J. D. Yakobi-Hancock et al.

Correspondence to: J. D. Yakobi-Hancock (jyakobi@dal.ca)

Supplement of Atmos. Chem. Phys., 14, 12307–12317, 2014
<http://www.atmos-chem-phys.net/14/12307/2014/>
doi:10.5194/acp-14-12307-2014-supplement
© Author(s) 2014. CC Attribution 3.0 License.



Supplement of

CCN activity of size-selected aerosol at a Pacific coastal location

J. D. Yakobi-Hancock et al.

Correspondence to: J. D. Yakobi-Hancock (jyakobi@dal.ca)

Supplementary Material

1 Conversion of particles' aerodynamic diameters ($d_{a,dry}$) to mobility diameters (d_m)

The inorganic components of the aerosol are determined by balancing the anionic and cationic charges of the ionic species that were reported by IC for the MOUDI size ranges (wet vacuum aerodynamic diameters) of 56 – 100 nm and 100 – 180 nm (see Table S1). For instance, if the concentrations of Na^+ and Cl^- were 1 mol/m^3 and 2 mol/m^3 , respectively, 1 mol/m^3 of NaCl would have been produced and the remaining Cl^- concentration would have been balanced by another cation such as K^+ to produce, for example, 1 mol/m^3 of KCl. It is assumed that through ionic balance $(\text{NH}_4)_2\text{SO}_4$, NaCl, NaNO_3 , KCl, $\text{K}_2\text{C}_2\text{O}_4$, KNO_2 , NaHSO_4 , and H_2SO_4 were produced, in that order.

In order to calculate the organic concentrations, the mass concentrations of ionic bearing constituents are subtracted from the total particle mass concentrations for each of the two size bins as determined from SMPS data and estimated densities (See Table S2), i.e. mass concentration of organics = total mass concentration – ionic mass concentration.

However, because the MOUDI and SMPS classify particles according to their wet aerodynamic diameters ($d_{a,wet}$) and dry mobility diameters (d_m), respectively, the MOUDI's $d_{a,wet}$ values are converted into the corresponding d_m values to allow for comparison of the size-resolved ionic and total particle mass concentrations. This is done in the following manner:

- 1) The aerosol ionic model (AIM, <http://www.aim.env.uea.ac.uk/aim/aim.php/>) is used to determine the volume of water in the aerosol at the average relative humidity during each time period (45% from August 17 – 19 and 40% from August 19 – 21, as measured using an Acurite 00891W3 relative humidity analyzer). These average relative humidities of air entering the trailer were assumed to approximate the outside RH since the trailer's doors were open during sampling. AIM is used by inputting the Na^+ , Cl^- , SO_4^{2-} , NH_4^+ , and NO_3^- concentrations (as measured by IC), with the unbalanced negative charge balanced using H^+ into the model and the assumption that the organics did not affect the amount of water present (Chang, 2011). A sensitivity study demonstrated that when the

amount of water present in the particles was doubled the resulting d_m values changed by less than 10 nm, which in turn validates the aforementioned assumption. Additionally, when propagating the error through these calculations, an error of $\pm 50\%$ was applied to the mass fraction of water in the particles as calculated by AIM.

- 2) To calculate the volume of the smallest and largest undried particles in each of the MOUDI's two size ranges, the undried aerosol is assumed to be spherical.
- 3) The undried aerosol's volume (found in step 2) is converted to mass using the density of the undried aerosol, i.e. the mass-weighted density of the wet aerosol (ρ_{wet}) at 50% RH, which is calculated according to Eq. S1:

$$\rho_{wet} = (\rho_{orgs})(f_{orgs}) + (\rho_{inorg,wet})(f_{inorg}), \quad (S1)$$

where ρ_{orgs} is the density of organics (assumed to be 1.3 g cm^{-3}), f_{orgs} is the mass fraction of organics in the aerosol (derived from the ACSM relationship of organic to sulfate mass concentrations and the IC sulfate concentrations), $\rho_{inorg,wet}$ is the density of the wet aerosol as calculated by AIM, and f_{inorg} is the fraction of inorganics in aerosol. To calculate f_{orgs} and f_{inorg} it is assumed that the aerosol contained both the inorganic species indicated by AIM and the organic species derived from the ACSM relationship of organic to sulfate mass concentrations.

- 4) The mass of solute in the undried aerosol is calculated by subtracting the mass of water in the undried aerosol (indicated by AIM) from the mass of undried aerosol that is found in step 3.
- 5) The mass of solute is converted to a volume using the mass-weighted density of the dry aerosol (ρ_{dry}). ρ_{dry} is calculated using the inorganic mass concentrations (found using IC measurements) and the organic mass concentrations (derived from the ACSM relationship of organic to sulfate mass concentrations and the IC sulfate concentrations).
- 6) The volume of solute is converted to a dry vacuum aerodynamic diameter ($d_{a,dry}$) by assuming that the dry particle is spherical.

7) $d_{a,dry}$ is converted to d_m using Eq. S2 (DeCarlo et al., 2004):

$$d_m = \frac{d_{a,dry}}{\sqrt{\frac{\rho_{dry}}{\rho_0 \chi_c}}}, \quad (\text{S2})$$

where ρ_{dry} is the mass weighted particle density, ρ_0 is the standard density (1.0 g cm^{-3}), and χ_c is the shape factor (assumed to be 1).

To propagate error through the above calculations, the uncertainties in the inorganic concentrations ($\pm 20\%$), ρ_{orgs} ($\pm 20\%$), the mass fraction of H_2O calculated by AIM ($\pm 50\%$), and the ACSM relationship of organic to sulfate mass concentrations ($\pm 20\%$), are used to calculate the error in d_m ($\pm 50\%$). Through this series of calculations, the d_m values of the two smallest size ranges of the MOUDI are determined to be: 42 (± 21) – 75 (± 38) nm and 78 (± 39) – 141 (± 71) nm.

2. References

Aljawhary, D., Lee, a. K. Y. and Abbatt, J. P. D.: High-resolution chemical ionization mass spectrometry (ToF-CIMS): application to study SOA composition and processing, *Atmos. Meas. Tech.*, 6, 3211–3224, doi:10.5194/amt-6-3211-2013, 2013.

Chang, R. Y.: Arctic Aerosol Sources and Continental Organic Aerosol Hygroscopicity by Arctic Aerosol Sources and Continental Organic Aerosol Hygroscopicity, University of Toronto, Ph.D. Thesis, 2011.

Christensen, S. I.: The Role of Temperature in Cloud Droplet Activation, North Carolina State University, Ph.D. Thesis, 2012.

DeCarlo, P. F., Slowik, J. G., Worsnop, D. R., Davidovits, P. and Jimenez, J. L.: Particle Morphology and Density Characterization by Combined Mobility and Aerodynamic Diameter Measurements. Part 1: Theory, *Aerosol Sci. Technol.*, 38, 1185–1205, doi:10.1080/027868290903907, 2004.

Petters, M. D. and Kreidenweis, S. M.: A single parameter representation of hygroscopic growth and cloud condensation nucleus activity, *Atmos. Chem. Phys.*, 7, 1961–1971, doi:10.5194/acp-7-1961-2007, 2007.

Table S1. Two day average ionic mass concentrations of the MOUDI's six particle size ranges (aerodynamic diameters) as measured by ion chromatography. The start date represents the first day and time (PDT) of each two day particle collection period.

Start Date	Particle Size (μm)	$\mu\text{g}/\text{m}^3$								
		Cl^-	NO_2^-	NO_3^-	SO_4^{2-}	$\text{C}_2\text{O}_4^{2-}$	Na^+	NH_4^+	K^+	MSA
Aug-13 12:03	>18	2E-03	1E-03	1E-03	8E-03	1E-03	2E-03	9E-04		2E-04
	0.56-18	1E-03		6E-04	3E-03		1E-03	1E-03		6E-05
	0.32-0.56	6E-02	5E-04	2E-02	7E-01	2E-02	2E-01	1E-01	1E-02	7E-02
	0.18-0.32	5E-04	5E-04	2E-03	2E-01	4E-03	8E-03	6E-02	4E-03	2E-02
	0.10-0.18	2E-03		9E-04	4E-02	1E-03	2E-03	1E-02	1E-03	4E-03
	0.056-0.10	7E-04		4E-04	6E-03	0E+00	8E-04	2E-03	9E-04	1E-03
Aug-15 12:22	>18	1E-03			1E-03		1E-03	7E-04		6E-05
	0.56-18	8E-04			7E-04	1E-03	1E-03	7E-04		3E-05
	0.32-0.56	2E-01		3E-02	3E-01	5E-03	2E-01	5E-02	5E-03	4E-02
	0.18-0.32	5E-04		1E-03	1E-01	3E-03	8E-03	4E-02	3E-03	2E-02
	0.10-0.18				4E-02		1E-03	1E-02	3E-03	6E-03
	0.056-0.10	5E-03		1E-03	9E-03	1E-03	2E-03	2E-03	1E-03	1E-03
Aug-17 12:44	>18	1E-03		1E-03	5E-03		1E-03	1E-03	0E+00	8E-04
	0.56-18	1E-03		2E-04	5E-03		1E-03	1E-03	1E-03	4E-04
	0.32-0.56	1E-02	9E-04	1E-02	1E+00	1E-02	2E-01	2E-01	9E-03	2E-01
	0.18-0.32	5E-04		1E-03	3E-01	2E-03	5E-03	5E-02	3E-03	5E-02
	0.10-0.18	3E-04		1E-04	7E-02		1E-03	2E-02	3E-03	1E-02
	0.056-0.10	5E-04		2E-04	6E-03		6E-04	2E-03		8E-04
Aug-19 12:42	>18	2E-03		3E-04	2E-03		2E-03	1E-03	1E-03	2E-04
	0.56-18	2E-03		4E-04	3E-03		2E-03	1E-03	9E-04	1E-04
	0.32-0.56	6E-01	2E-03	4E-02	1E+00	2E-02	6E-01	2E-01	2E-02	2E-01
	0.18-0.32	5E-04	4E-04		4E-01	2E-03	2E-02	9E-02	2E-03	4E-02
	0.10-0.18	7E-04		5E-04	5E-02	1E-03	2E-03	1E-02		8E-03
	0.056-0.10	2E-03		4E-04	6E-03		2E-03	2E-03		1E-03
Aug-21 13:51	>18	1E-03		1E-03	3E-03		8E-04	1E-03		2E-04
	0.56-18	8E-04		1E-03	3E-03		5E-04	1E-03		2E-04
	0.32-0.56	2E-02	6E-04	1E-02	5E-01	8E-03	1E-01	1E-01	4E-03	5E-02
	0.18-0.32	9E-04	5E-04	2E-03	2E-01	2E-03	5E-03	5E-02	2E-03	2E-02
	0.10-0.18	5E-04		2E-03	4E-02	1E-03	1E-03	1E-02	2E-03	3E-03
	0.056-0.10	2E-03			9E-03	9E-04	1E-03	3E-03	8E-04	7E-04

Table S2. Assumed densities (ρ) of inorganic species.

Compound	ρ (g cm⁻³)
(NH ₄) ₂ SO ₄	1.77
H ₂ SO ₄	1.84
NaCl	2.16
KCl	1.98
NaNO ₃	2.26
NaHSO ₄	2.74
KNO ₂	1.91
K ₂ C ₂ O ₄	2.13
MSA ⁻	1.48

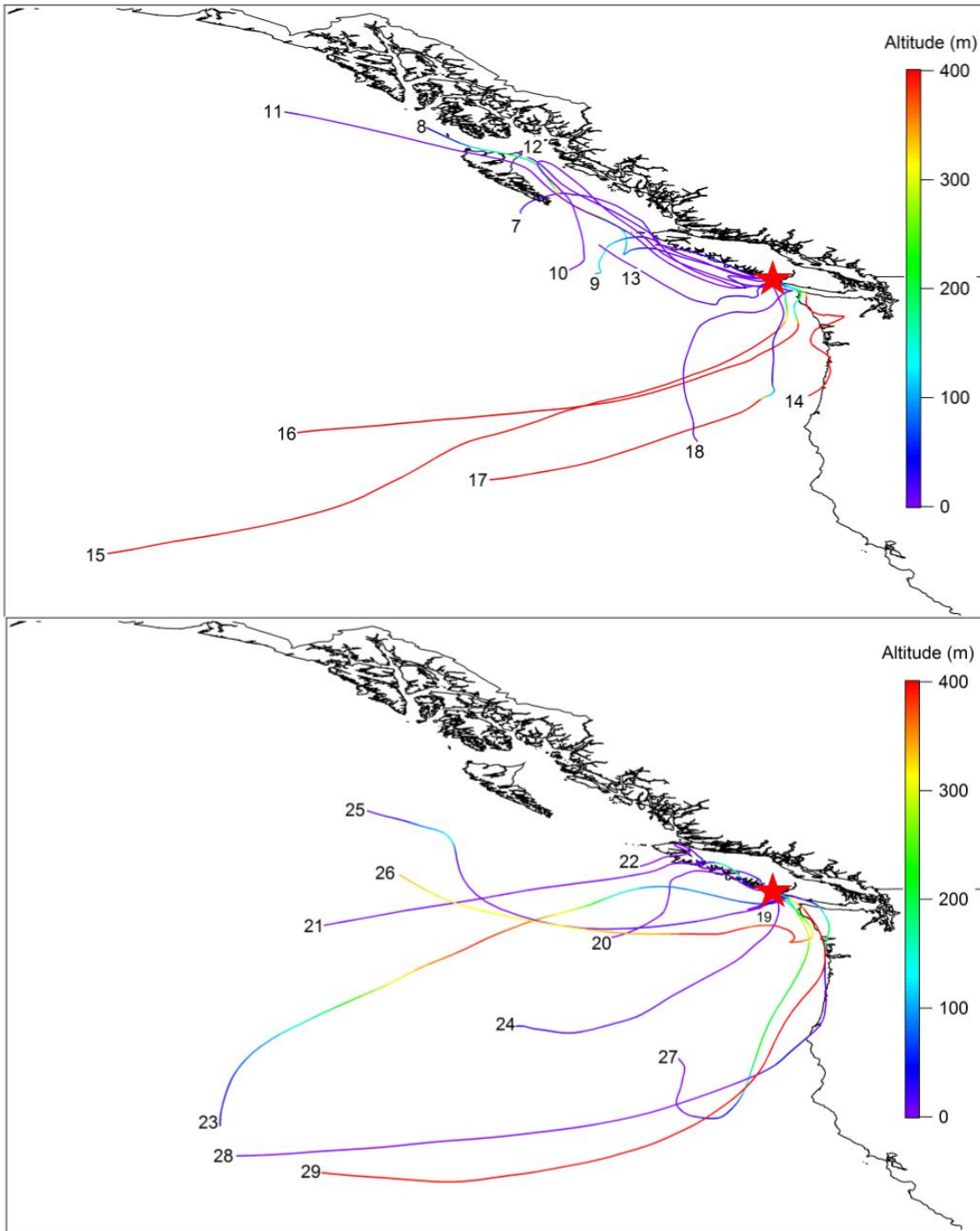


Figure S1. Examples of air masses that were seen throughout the entire campaign, generated using the NOAA Air Resources Laboratory-HYSPLIT program. Each air mass arrived in Ucluelet (red star) at 12:00 (PDT) on each day of the campaign, where the number indicates the date of arrival in August. The air masses have been classified according as types (a) August 7 – 12, (b) August 14 – 16, 23, (c) August 13, 18 – 20, and (d) August 21 – 22, as described in Sect. 3.1.

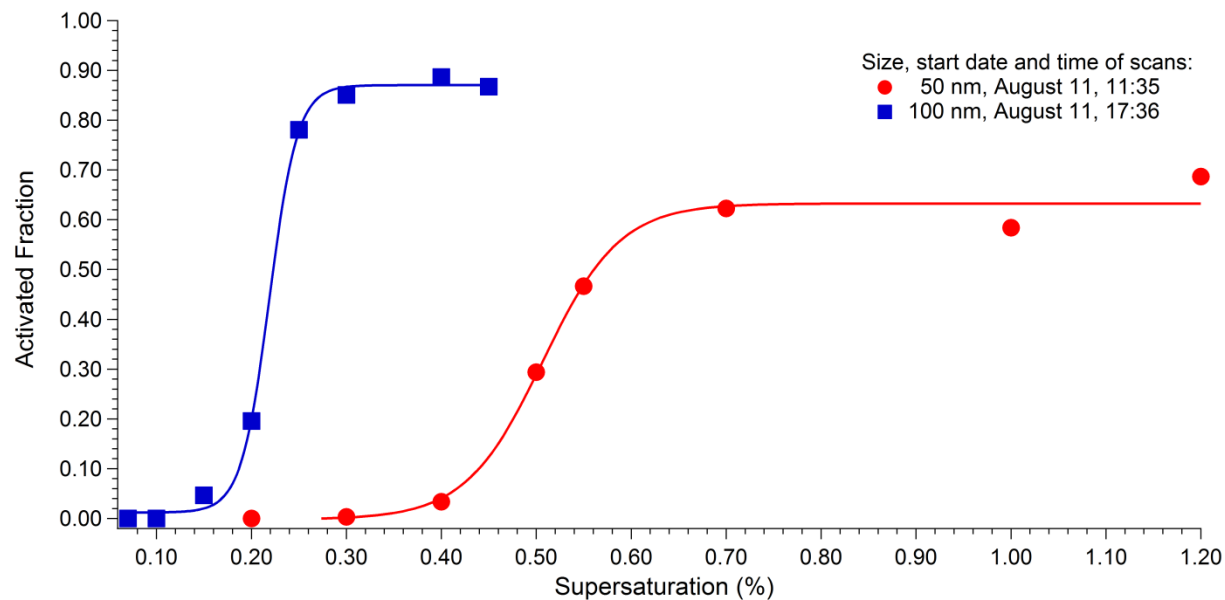


Figure S2. Examples of activated fraction versus supersaturation (%) curves for 50nm (red circles) and 100nm particles (blue squares), where the scans' dates and times are in PDT.

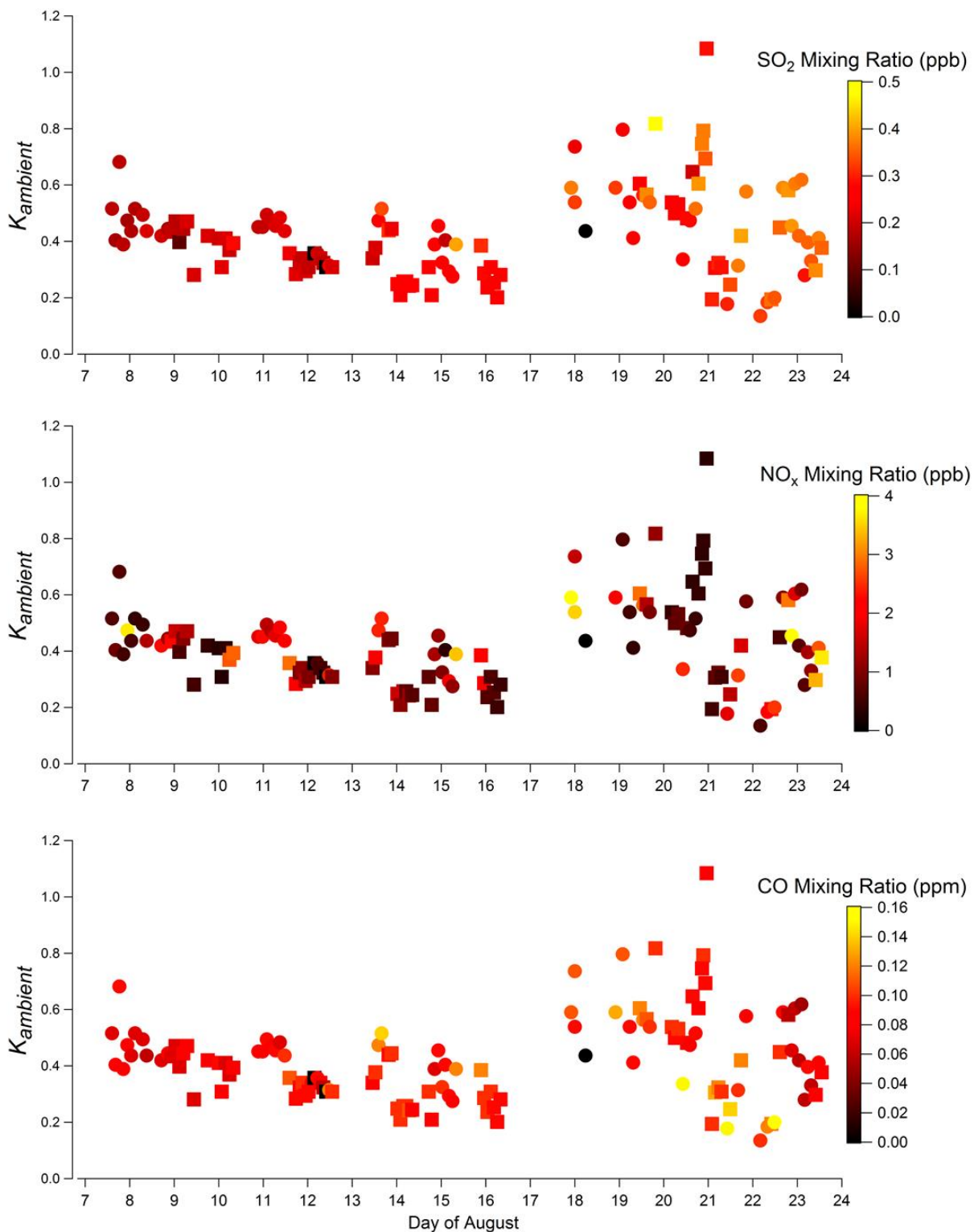


Figure S3. Time series (PDT) of $\kappa_{ambient}$ colour coded according to the corresponding SO₂ (top), NO_x (middle), and CO (bottom) mixing ratios. The relative error in $\kappa_{ambient}$ is $\pm 37\%$.

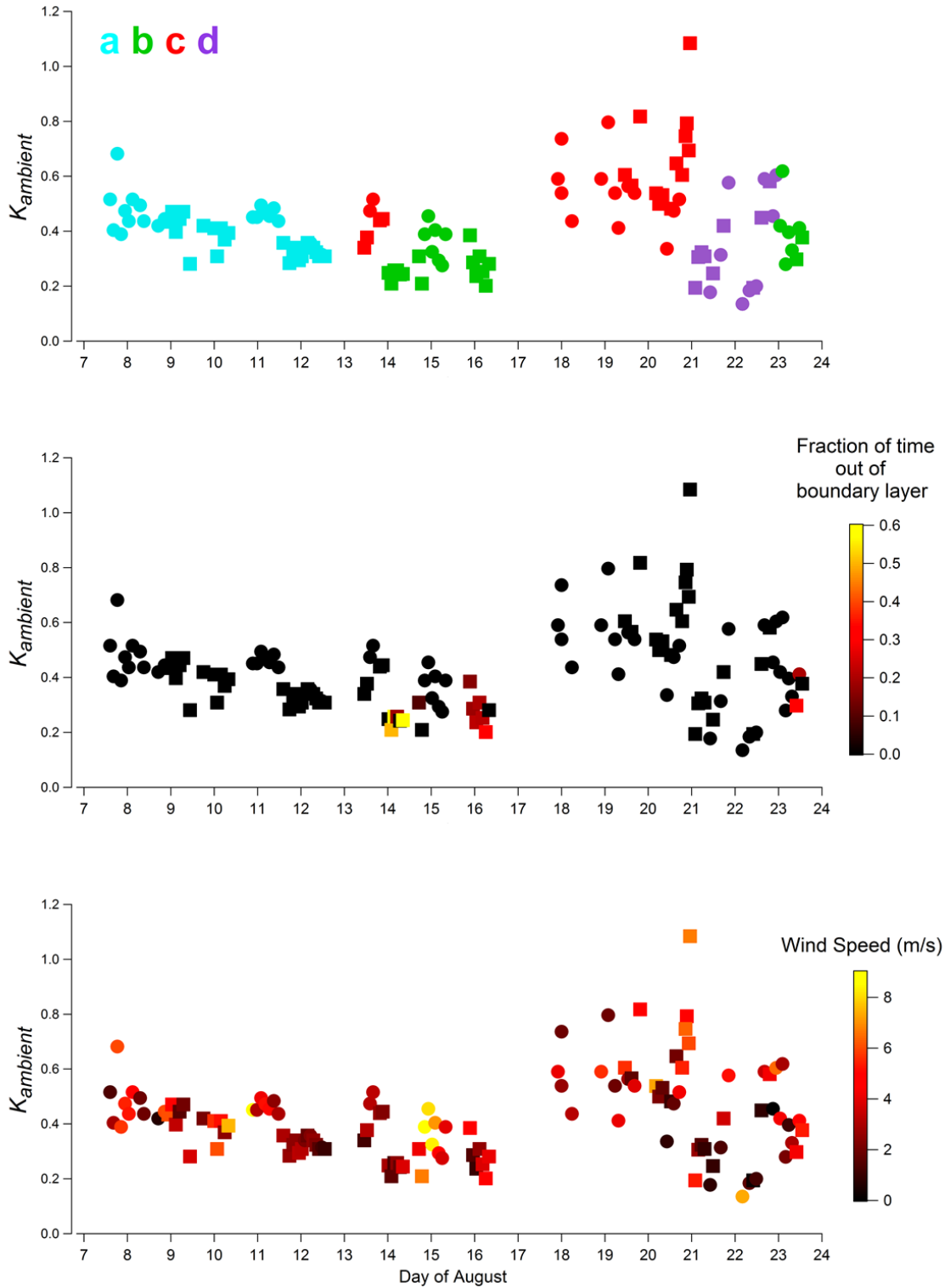


Figure S4. Time series (PDT) of κ_{ambient} colour coded according to the corresponding air mass origins (top), the fraction of time that the air masses (72 hour back trajectories) were above the marine boundary layer i.e. above 1000 m (middle), and the average wind speed (bottom). The air masses have been classified as type a, b, c, and d, according to the classification scheme described in Sect. 3.1. The relative error in κ_{ambient} is $\pm 37\%$.